Data supplement for Sylvester et al., Neonatal Brain Response to Deviant Auditory Stimuli and Relation to Maternal Trait Anxiety. Am J Psychiatry (doi: 10.1176/appi.ajp.2020.20050672)

SUPPLEMENTAL METHODS/RESULTS

Recruitment Details and Additional Sample Characteristics

We recruited participants from a separate study at Washington University: the Early Life Adversity, Biological Embedding, and Risk for Developmental Precursors of Mental Disorders (eLABE) study. The eLABE study recruited participants during the 2nd or 3rd trimester of pregnancy from two outpatient obstetrics clinics at Washington University. Although there was no effort to select participants with any particular risk factors (i.e., it was a convenience sample), the average area deprivation index (ADI) was 72.0. This ADI is a publicly available metric that calculates census block disadvantage based on home address using characteristics such as average home value, educational attainment, poverty prevalence, and household crowding and is reported as a national percentile (1). Higher values indicate greater disadvantage, and an average of 72.0 indicates relatively high disadvantage.

Parents were approached during the neuroimaging visit for eLABE to ask whether they would be willing to participate in the current study. Of the 387 participants who were scanned for eLABE, approximately 50 were approached between May 2018 and May 2019 for recruitment into the current study. To be eligible for invitation, participants had to have access to transportation, and offspring had to have been born full-term (36 weeks gestation or greater). Table S1 compares participants from the eLABE study who did versus who did not participate in the current study. Anatomic MR images from the parent eLABE study were reviewed by a neuroradiologist (J.S.S.) and pediatric neurologist (C.D.S.). Subjects were not invited to

participate in the current study if they had evidence of brain injury. Additional inclusion criteria for the current study included speaking English and age 18 years or older. Exclusion criteria included pregnancy complications, known fetal abnormalities including intrauterine growth restriction, and preterm birth (<36 weeks gestational age).

Assessment of Maternal Symptoms and Socioeconomic Status (SES)

Depression was assessed using the Edinburgh Postnatal Depression Scale (2) at each trimester and averaging over all available assessments. Total perceived stress was measured with the Perceived Stress Scale (3) at each trimester and averaging over all available assessments. State anxiety was measured with the state subscale of the STAI (4), the STAI-S. The STAI-S was completed by 32 participants within a 5-week period following birth and 7 participants within an 8-week period following the child's first birthday. Socioeconomic status (SES) was assessed with the Area Deprivation Index (ADI) as determined by home address at the time of birth, described above (1).

fMRI Data Collection and Acquisition Parameters

After feeding, the infant was swaddled and positioned in a head-stabilizing vacuum fix wrap (5). A nurse familiar with neonate transport and resuscitation was present at all MRI scans. Heart rate and blood oxygenation were measured continuously throughout all scans, and infants were monitored visually via video. Based on visual monitoring through a camera, infants slept through scans as indicated by eye closure and minimal movements.

As part of the eLABE study, a T2-weighted image (sagittal, 208 slices, 0.8 mm isotropic resolution, TE=563 ms, TR=4500 ms) was collected. For the task-based fMRI, functional

imaging was performed using a blood-oxygen-level dependent (BOLD) gradient-recalled echo-planar multiband (MB) sequence (72 slices, 2.0 mm isotropic resolution, TE=37 ms, TR=800 ms, MB factor=8). Spin-echo field maps were obtained (at least one anterior→posterior and one posterior→anterior) during each session with the same parameters.

fMRI Pre-Processing

fMRI preprocessing included correction of intensity differences attributable to interleaved acquisition, bias field correction, intensity normalization of each run to a whole brain mode value of 1000, linear realignment within and across runs to compensate for rigid body motion, and linear registration of BOLD images to the adult Talairach 3 mm isotropic atlas, via the T2-weighted image. Field distortion correction was peformed by using the FSL TOPUP toolbox (http://fsl.fmrib.ox.ac.uk/fsl/fslwiki/TOPUP). Statistical analyses were performed within a brain mask that included all gray matter voxels in the neonatal brain, cortical and subcortical.

General Linear Modeling of BOLD Activity

Baseline and linear trend terms were included for each run. Neural response to the background scanner noise is expected to be at steady state throughout the scan, and therefore it was not explicitly coded into the GLM; response to the background scanner noise is implicitly represented by the baseline and linear trend terms. Responses to deviant sounds were modeled without any assumption about the hemodynamic response function (HRF), which differs in infants compared to adults (30). The auditory response was modeled by using separate finite impulse response (FIR) regressors (34) for each of the 40 BOLD frames following white noise onset (40 frames × 0.8 seconds yielding TR = 32 seconds modeled). The regressors were derived

for each subject for each voxel and entered into the 2nd level statistical models described in the main text.

Multiple Comparisons Correction

The whole-brain maps included statistical tests for main effect of timepoint from the first analysis and the interaction between timepoint and maternal anxiety in the second analysis. These maps were multiple comparisons corrected. We used the latest recommendation to measure study-specific auto-correlation parameters on the basis of the pre-processed, smoothed data, using 3dFWHMx from AFNI (6, 7). These auto-correlation parameters were then used in simulations with 3dClustSim from AFNI within the gray matter mask to derive family-wise cluster-based error rates. To avoid an unacceptable level of false positives, we required each voxel to be significant at $p<0.001$ ($z=3.3$); 3dClustSim determined that a cluster size of 28 voxels in 3×3×3mm isotropic atlas space (756 mm^3) at this threshold was required to achieve a whole-brain cluster-wise error rate of $p<0.01$, using the parameter NN=1 (meaning that voxel faces must touch to be counted in the same cluster).

Region-of-Interest and Timecourse Derivation

Regions-of-interest (ROIs) were derived from each multiple-comparison corrected image using a peak-finding algorithm. Spheres of diameter 10 mm were generated around peaks greater than $z=3.3$ and spheres closer than 10 mm to each other were consolidated into one ROI. ROIs were clipped such that all voxels $|z|>3.3$; ROIs smaller than 28 voxels were discarded. Timecourses were generated for each ROI, and ROIs were rejected if the initial or final frame demonstrated a modeled response that was greater than |0.2%| BOLD change. Such high activity

simultaneous with the onset of the auditory stimulus is not physiologically possible due to the delayed onset of the BOLD response and suggests either movement-related artifact or poor modeling of the baseline. Seven ROIs were excluded from the main effect of time analysis based on this criterion. The corresponding statistical clusters were removed from the maps displayed in each statistical image in this manuscript. For display purposes, timecourses were averaged across all voxels within a ROI.

Network Characterization

The statistical maps for the current study were computed in Talairach volume space (35), and the results were projected to a standardized surface using Workbench tools (36, 37). This standardized surface was created from an average of 12 full-term infants and has been spherically registered to the fsLR_32k standard surface space used in adults (38). Thus, there is node-to-node correspondence between the infant and standard adult surfaces. We applied adult functional brain network definitions (39) publicly available in this common surface space to the neonatal statistical maps (see Figures S5 and S6). We then computed the percentage of surface area of each adult-defined network in which activity in neonates was significantly modulated following the auditory stimulus (Figure 2 from main text).

Distribution of Maternal Anxiety Scores and Median-Split Analysis

Figure S2 provides a histogram of maternal trait anxiety scores. The initial distribution did not follow a normal distribution (Shapiro-Wilks (41)=0.938, $p<0.03$), which appeared to be related to two mothers with high trait anxiety scores (53 and 51) as well as some evidence of a bimodal distribution. Thus, we repeated the primary analysis examining the interaction between

timepoint and maternal anxiety but treating anxiety as a categorical variable using a median split (30 or lower versus 31 or higher). Results were nearly identical as seen in Figures S7 and S8. In addition, in the primary analysis in the main text, the maternal trait anxiety scores of the two women with high scores (51 and 53) were winsorized to the next highest value (41).

Responses to Stimuli Occurring Early, Middle, and Late within each Run

Brain regions responding to salience might be expected to exhibit the highest activity when stimuli are the most unexpected (8). Therefore, we tested whether regional brain activity in response to the auditory stimuli varied as a function of time, contrasting responses from the early, middle, and late portion of each fMRI run. Within each BOLD run, we considered the first 8 stimuli as 'early', the next 8 stimuli as 'middle', and the last 8 stimuli as 'late'. We created a new voxelwise GLM with the same characteristics as above, except that we separately modeled responses for early, middle, and late auditory stimuli (each modeled response consisting of 40 FIRs, as above). Timecourse estimates for early, middle, and late auditory stimuli were averaged across each of the ROIs from the main effect of time analysis. For each ROI, we then computed a repeated measures ANOVA with timepoint (1-40 frames after the stimulus onset), epoch (early, middle, late), and timepoint by epoch interaction as factors. In 105 (61%) of the ROIs, there was a significant interaction between timepoint and epoch, indicating that the activity modulation varied as a function of epoch. In each case, activity was highest for early stimuli, lowest for late stimuli, and generally intermediate for middle stimuli. Example timecourses for stimuli in early, middle, and late epochs are illustrated in Figure S3.

In a series of exploratory analyses, we also tested whether the relation between maternal trait anxiety and neonatal brain activity in response to the auditory stimuli varied depending on

whether the stimuli were presented in the early, middle, or late epoch. First, we computed a fully factorial whole-brain repeated measures ANOVA with timepoint (1-40 frames after the stimulus onset), epoch (early, middle, late), and maternal trait anxiety (continuous score on STAI-T) as factors. Figure S12 illustrates a whole-brain map of regions showing a three-way interaction between time, epoch, and maternal trait anxiety. In addition to this analysis, we also computed 3 different whole-brain repeated measures ANOVAs for the interaction between time and maternal anxiety, separately for each epoch. These analyses are illustrated in Figure S13.

Comparison of Participants with Shorter Versus Longer BOLD Runs

As described in the main text, the scans were 5.7 minutes in length for the first 37 infants and 6.7 minutes in length for the next 8 infants. In the first 37 infants, the scans ended after the last auditory stimulus, while in the last eight infants an additional 56s of scan time was included in which no white noise stimuli were presented. We had added in the extra time to improve modeling, but exploratory analyses in the 8 subjects with the extra time found no meaningful differences in modeling of events when this extra time was included versus excluded (Figure S14). To assess, for each of the 8 subjects, we computed 2 separate GLMs that modeled early, middle, and late auditory stimuli (see preceding section). One of these 2 GLMs included all data for each subject; the second GLM for each subject removed the extra 56s of collected BOLD data. Figure S14 illustrates the main effect of time for the early, middle, and late epochs in the 8 subjects in question; using either the full dataset or the dataset with the last 56s removed. This figure demonstrates a very small difference for the late stimulus response and almost no effect of estimates of early and middle stimulus responses.

Assessment of Infant Head Movements

Frame-to-frame head movement was computed using framewise displacement (FD) as

previously described (9). Note that FD was computed in Talairach space, which scales the brain by a factor of approximately 1.6 in each dimension. Thus, FD values reported in the current study represent smaller actual movements (in real space) compared to equivalent FD values reported in adult studies. As above, frames with greater than 0.9 FD were excluded from analyses. Overall, movements were minimal, as median FD before frame censoring was 0.31 and median FD after frame censoring was 0.12. An FD cutoff of 0.9 is the standard for task-based fMRI studies, which have different trade-offs between power and noise compared to resting-state fMRI studies (10). When using a cutoff of FD<0.2, we retained an average of 28 minutes of data per subject, compared to an average of 31 minutes of data per subject with an FD cutoff of 0.9. Figure S11 shows the interaction between time and maternal trait anxiety (equivalent to Figure 3 in the main text) when only using data with FD<0.2.

To determine whether movements occurred systematically in relation to the onset of the sounds, we computed the average FD for each participant for each frame 1-40 following the onset of the sound. We then computed a repeated-measures ANOVA testing whether FD varied over these 40 different timepoints and found no significant relationship as reported in the main text.

Control for Confounding Variables

For the 172 ROIs with significant activity modulations following the sound onset, we ran additional post-hoc models to test whether the reported results survived when additionally including average FD and number of retained frames after censoring; only one region did not survive as reported in Table S3. For the 86 ROIs in which activity modulations following sound onset varied significantly as a function of maternal anxiety, we ran additional models testing whether reported results survived when controlling for FD, number of retained frames, maternal

state anxiety (STAI-S), maternal depression (EPDS), maternal stress (PSS), socioeconomic status (ADI), infant sex, gestational age at birth, age at scan, birthweight. Covariates were tested one at a time and all models were fully factorial. The results of controlling for each covariate for each ROI are listed in Tables S3 and S4.

Activity in Auditory Networks

To test for evidence of positive activity changes in the auditory network, we computed a magnitude of activity for each infant for each ROI within the auditory network from the main effect of time analysis (the regions listed in Table S3). Magnitudes were computed by taking the dot product of an individual neonate's timecourse from an individual region with a 'canonical' neonatal timecourse computed from this dataset by averaging over all infants and all regions. Figure S15 plots a histogram of the maximum magnitude of activation across the auditory ROIs for each infant; based on this metric, 42 of the 45 infants showed a positive magnitude of activity in an auditory network ROI.

	Participated in Current Study (n=45)			Did Not Participate in Current Study (n=342)			Statistical Group Difference
	n	Mean	SD	n	Mean	SD	
Trait Anxiety		31.17	7.49		33.46	9.99	t= -1.42 p= .158
State Anxiety		28.46	7.56		29.88	9.95	t= -.881 p= .379
Depression		4.02	3.11		5.07	4.40	t= -1.52 p= 0.129
Stress, Mean		12.77	5.73		13.83	6.70	t= -.991 p= .322
Sex Male Female	 18 27			 194 148			 **χ^2= 4.49** **p= 0.034**
GA in weeks at Birth		38.2	1.03		37.89	2.13	t= .886 p= .376
Birthweight in grams		3115	488.41		3139	620.44	t= -.254 p= .800
SES		72.00	22.46		69.16	25.06	t= .724 p= .469
Race Black White Other	 29 16 0			 208 127 11			 χ^2= .220 p= .639 χ^2= .043 p= .837 χ^2= 1.43 p= .233

TABLE S1. Comparison of children from the parent eLABE study who did versus who did not participate in the current study. Trait and state anxiety were measured with the State-Trait Anxiety Inventory (STAI). Depression was measured with the Edinburgh Postnatal Depression Scale (EPDS). Stress was measured with the Perceived Stress Scale (SES). SES was measured with the Area Deprivation Index (ADI). Participants could identify with more than one race. GA = gestational age.

	Trait Anxiety	State Anxiety	Depress-ion	Stress	Sex	GA Birth	Scan Age	Birth Weight	SES	Race	FD
State Anxiety	**r= .706 p< .001**										
Depression	**r= .500 p= .001**	**r= .497 p= .001**									
Stress	**r= .604 p< .001**	**r= .350 p= .025**	**r= .559 p< .001**								
Sex	t= -1.19 p= .242	t= -.410 p= .684	t= -.404 p= .688	t= .254 p= .801							
GA at Birth	r= .055 p= .732	r= .129 p= .423	r= .026 p= .869	r= -.183 r= .240	t= -.945 p= .350						
Scan Age	r= .082 p= .612	r= -.080 p= .621	r= -.294 p= .056	r= .030 p= .847	t= .252 p= .802	**r= -.427 p= .003**					
Birthweight	r= -.158 p= .324	r= -.023 p= .885	r= -.142 p= .363	r= -.296 p= .054	t= 1.74 p= .089	**r= .370 p= .012**	r= -.119 p= .437				
SES	r= -.069 p= .668	r= -.209 p= .190	r= -.120 p= .445	r= .027 p= .863	t= -1.09 p= .283	r= .006 p= .970	r= -.243 p= .107	**r= -.472 p= .001**			
Race	t= .212 p= .833	t= .087 p= .931	t= .035 p= .972	t= -.704 p= .485	χ^2= .07 p= .799	t= .954 p= .345	t= .253 p= .801	**t= 3.32 p= .002**	**t= -5.30 p< .001**		
FD	r= -.208 p= .191	r= -.139 p= .385	r= -.067 p= .670	r= .076 p= .627	t= -.296 p= .769	r= -.044 p= .773	r= -.006 p= .966	r= -.053 p= .732	r= .129 p= .397	t= -1.01 p= .320	
N Retained Frames	r= -.224 p= .160	r= -.043 p= .789	r= -.032 p= .840	r= -.071 p= .653	t= -.151 p= .881	r= -.160 p= .292	r= .041 p= .788	r= -.024 p= .873	r= -.261 p= .083	t= 1.57 p= .124	r= -.291 p= .053

TABLE S2. Zero order relations among covariates described in the current study. Pearson's correlations are calculated for relating pairs of continuous variables, two-sample t-tests are used for relating categorical variables to continuous variables, and chi-square tests are used to relate categorical variables to each other. For categorical variables, the coding was as follows: sex (males=1, females=2), race (White=1, African American=2). Significant relations (p<.05) are bolded. State and trait anxiety were measured with the State-Trait Anxiety Inventory (STAI). Depression was measured with the Edinburgh Postnatal Depression Scale (EPDS). Stress was measured with the Perceived Stress Scale. GA = gestational age; SES = socioeconomic status, computed with the Area Deprivation Index (ADI); FD = framewise displacement, a measure of movement during scanning; N Retained Frames = number of retained BOLD frames after censoring.

Regions with Significant Activity Modulations Following Deviant Sounds

Peak in Adult Talairach Space							
x	**y**	**z**	**Location**	**Adult Network**	**Peak z**	**Volume (mm^3)**	**Not Sig. (p>0.001) After Motion Control**
-58	-34	6	STG	Auditory	8.2	1701	
-56	-42	13	STG	Auditory	9.2	2268	
-56	-21	13	TTG	Auditory	10.8	2916	
-50	-36	24	IPL	Auditory	7.3	2322	
-48	-49	24	SMG	Auditory	6.0	1188	
-33	-32	22	Insula	Auditory	13.9	2754	
25	-22	20	Claustrum	Auditory	8.8	2457	
32	-35	23	Insula	Auditory	8.5	2592	
47	-43	23	IPL	Auditory	9.6	2565	
50	-12	17	PostCent	Auditory	12.7	2754	
-56	-44	31	SMG	CingOperc	5.9	2025	
-51	-9	9	STG	CingOperc	15.2	3078	
-48	1	0	STG	CingOperc	15.4	3726	
-38	12	8	Insula	CingOperc	12.0	3510	
-37	-16	-6	Claustrum	CingOperc	9.0	1512	
-35	-4	13	Insula	CingOperc	13.6	3861	
-17	-39	32	Cing	CingOperc	7.1	1215	
-10	-49	49	Precuneus	CingOperc	8.3	1917	
-8	-10	49	MedFront	CingOperc	15.6	2943	
-7	2	49	MedFront	CingOperc	14.5	2403	
-3	-16	33	Cing	CingOperc	13.5	2511	
-2	-55	51	Precuneus	CingOperc	9.7	1998	
-2	2	40	Cing	CingOperc	16.9	2727	
-1	-6	21	Cing	CingOperc	8.9	2781	
6	2	50	MedFront	CingOperc	15.8	2754	
7	-6	42	Cing	CingOperc	16.5	3051	
7	-4	61	MedFront	CingOperc	13.1	2781	
16	-41	36	Cing	CingOperc	9.6	1809	
26	10	17	Claustrum	CingOperc	8.8	1080	
33	20	9	Insula	CingOperc	8.7	2700	
35	-5	16	Insula	CingOperc	11.8	3051	
38	-1	-2	Insula	CingOperc	6.6	1728	
39	-18	-3	Insula	CingOperc	7.2	1134	
43	8	3	Insula	CingOperc	11.8	2754	
53	0	3	STG	CingOperc	10.2	2781	
-55	-24	-13	MTG	Default	10.3	1728	
-32	6	53	MFG	Default	9.4	2025	
-26	5	43	MFG	Default	8.6	2025	
-24	24	55	MFG	Default	5.7	1404	
-5	-66	11	PostCing	Default	8.1	1647	
-5	-48	9	PostCing	Default	12.5	2619	
-3	35	45	SFG	Default	10.7	3105	
-3	37	12	AntCing	Default	6.7	1971	
-2	-41	17	PostCing	Default	11.9	2484	
-2	32	29	Cing	Default	9.7	2943	
-2	44	29	MedFront	Default	7.7	1971	
4	-52	39	Precuneus	Default	5.8	1269	

8	-43	7	PostCing	Default	16.1	3510	
9	32	55	SFG	Default	8.7	1701	
11	-54	24	PostCing	Default	8.7	1836	
11	35	42	MedFront	Default	8.3	2430	
24	15	41	MFG	Default	5.0	1134	
50	-12	-17	MTG	Default	8.4	1350	
51	-23	-13	MTG	Default	10.6	2295	
-47	-35	43	IPL	DorsalAttn	8.2	1431	
-27	-13	54	PreCent	DorsalAttn	13.3	3591	
-20	-4	64	SFG	DorsalAttn	10.3	2241	
2	-71	59	Precuneus	DorsalAttn	8.5	1674	
19	-73	41	Precuneus	DorsalAttn	6.8	1296	
20	-8	61	MFG	DorsalAttn	11.4	2754	
30	-5	53	MFG	DorsalAttn	10.3	3429	
-43	-1	38	PreCent	FrontoPar	12.6	3510	
-32	-1	30	PreCent	FrontoPar	10.8	3429	
-1	18	56	SFG	FrontoPar	11.3	3456	
0	-88	34	Cuneus	FrontoPar	9.8	2052	
35	10	26	IFG	FrontoPar	8.8	1728	
36	19	39	MFG	FrontoPar	7.5	2295	
45	14	27	MFG	FrontoPar	9.7	1782	
47	3	36	PreCent	FrontoPar	13.0	2565	
-4	-23	26	Cing	MedPar	12.2	2727	
6	-38	22	PostCing	MedPar	12.3	2538	
7	-22	29	Cing	MedPar	13.1	2403	
-40	-32	53	PostCent	MortorHand	9.6	1458	
-32	-45	62	PostCent	MortorHand	7.7	1620	
-31	-29	58	PreCent	MortorHand	11.4	1593	
-25	-22	19	Claustrum	MortorHand	15.1	3699	
-21	-20	66	PreCent	MortorHand	10.4	2457	
-18	-34	67	PostCent	MortorHand	7.6	918	
-17	-23	45	Cing	MortorHand	11.1	3213	
-7	-32	46	Precuneus	MortorHand	13.7	3024	
-5	-22	43	ParaCent	MortorHand	14.8	2484	
-3	-19	61	MedFront	MortorHand	13.8	3078	
10	-23	39	Cing	MortorHand	13.3	3375	
11	-15	60	MedFront	MortorHand	12.1	2916	
13	-60	62	SPL	MortorHand	6.5	945	
29	-21	58	PreCent	MortorHand	8.9	2862	
40	-13	22	Insula	MortorHand	9.7	2295	
-49	-12	20	PostCent	MotorMouth	12.5	3132	
-47	-14	39	PreCent	MotorMouth	16.2	3186	
-33	-18	36	PreCent	MotorMouth	14.9	3780	
38	-10	42	PreCent	MotorMouth	10.3	3051	
44	-13	35	PreCent	MotorMouth	10.7	2511	
54	-4	28	PreCent	MotorMouth	9.2	2538	
61	-16	23	PostCent	MotorMouth	7.6	1674	
-44	-47	-39	Tonsil	NA	5.6	1080	
-30	-38	-50	Cerebellum	NA	6.5	1188	
-29	-60	-38	Tonsil	NA	4.8	945	
-23	-13	-2	Lent	NA	13.3	3186	
-20	-42	8	PHG	NA	9.9	1620	
-19	-38	-52	Cerebellum	NA	6.6	1431	

-18	-4	10	Lent	NA	7.3	1998	
-9	-21	14	Thalamus	NA	11.9	2781	
-6	-34	6	PHG	NA	13.0	2403	
-4	-26	-7	Brainstem	NA	7.7	2349	
-2	-86	-30	Pyramis	NA	7.8	2025	p=0.001
1	-18	-32	Brainstem	NA	9.3	2673	
2	-9	-8	Thalamus	NA	6.0	783	
3	-29	10	Thalamus	NA	13.9	2943	
5	4	2	Caudate	NA	6.3	918	
10	-41	-18	Culmen	NA	5.6	783	
11	-18	2	Thalamus	NA	8.4	1944	
12	-84	-29	Pyramis	NA	9.6	1917	
17	-11	-1	Lent	NA	11.4	2052	
26	-10	24	Lent	NA	8.7	2052	
26	1	28	Caudate	NA	7.6	2025	
30	-9	-5	Lent	NA	8.3	2268	
39	-44	-46	Tonsil	NA	8.3	2160	
39	-15	-21	Fusiform	NA	6.4	1053	
47	-55	-28	Tuber	NA	6.7	1296	
57	0	-27	MTG	NA	8.7	1026	
-17	3	55	MedFront	ParOccip	10.8	2538	
-12	-36	-23	Culmen	ParOccip	7.3	1215	
21	-35	-28	Tonsil	ParOccip	13.4	3483	
-10	12	36	Cing	Salience	15.2	3078	
-8	22	31	Cing	Salience	11.0	2916	
1	10	27	Cing	Salience	13.9	3375	
-43	-11	-13	MTG	Unassigned	7.3	1782	
-36	8	-13	Insula	Unassigned	8.6	2646	
-34	7	-29	STG	Unassigned	8.2	1674	
-21	-29	-9	PHG	Unassigned	11.3	2484	
-21	-1	-11	PHG	Unassigned	7.7	1512	
-21	5	-38	Uncus	Unassigned	15.0	2241	
-17	-26	-29	Culmen	Unassigned	10.9	2565	
-17	-15	-15	PHG/Hipp	Unassigned	9.3	2835	
-9	-36	-10	Culmen	Unassigned	8.9	1404	
17	-29	-8	PHG	Unassigned	9.6	2376	
17	-8	-20	PHG/Amyg	Unassigned	6.7	1755	
22	-19	-15	PHG/Hipp	Unassigned	7.7	1944	
29	-33	-7	PHG/Hipp	Unassigned	8.2	1917	
30	18	-10	IFG/Insula	Unassigned	4.9	810	
31	5	-13	IFG/Insula	Unassigned	7.4	1917	
33	-3	-32	Uncus	Unassigned	7.9	2376	
37	-44	-30	Culmen	Unassigned	10.5	3186	
38	-72	11	MOG	Unassigned	8.2	1836	
38	5	-26	STG	Unassigned	9.6	2106	
41	19	-7	IFG	Unassigned	7.7	2025	
46	3	-13	STG	Unassigned	8.4	2052	
-58	-17	-5	MTG	VentAttn	9.2	2349	
-57	-50	3	MTG	VentAttn	5.5	1242	
-55	-2	-14	MTG	VentAttn	7.1	1107	
-46	-56	7	MTG	VentAttn	5.9	837	
-10	-2	62	MedFront	VentAttn	14.3	2160	
7	10	65	SFG	VentAttn	12.7	2268	

41	-27	3	STG	VentAttn	6.4	1215	
44	-44	1	MTG	VentAttn	8.1	2916	
51	-52	20	STG	VentAttn	10.3	1836	
52	-8	-4	STG	VentAttn	9.2	2187	
58	-38	4	MTG	VentAttn	8.3	1566	
58	-25	4	STG	VentAttn	8.1	2376	
-21	-43	-6	PHG	Visual	7.4	1350	
-17	-70	3	Ling	Visual	8.5	2646	
-10	-65	-13	Ling	Visual	6.5	918	
-10	-55	1	Ling	Visual	10.5	2349	
-10	-41	-1	PHG	Visual	12.8	1836	
-8	-76	-15	Ling	Visual	7.9	1512	
-6	-46	-11	Cerebellum	Visual	8.3	1080	
3	-91	-13	Ling	Visual	6.6	1107	
5	-71	-1	Ling	Visual	12.8	3240	
6	-77	-19	Ling	Visual	8.8	2673	
13	-64	-23	Declive	Visual	9.2	1674	
19	-75	24	Cuneus	Visual	4.9	1107	
21	-73	-20	Ling	Visual	7.8	1755	
23	-61	-26	Culmen	Visual	5.7	837	
24	-60	1	Ling	Visual	9.9	2484	
29	-46	-7	PHG	Visual	7.1	1485	
37	-58	-26	Ling	Visual	6.9	1296	
39	-70	-8	MOG	Visual	7.0	1242	

TABLE S3. Regions with significant activity modulation following the onset of the deviant sound. IPL: inferior parietal lobule; MFG: middle frontal gyrus; STG: superior temporal gyrus; IFG: inferior frontal gyrus; MTG: middle temporal gyrus; TTG: transverse temporal gyrus; Ant: anterior; Post: posterior; Cing: cingulate gyrus; MOG: middle occipital gyrus; PreCent: pre-central gyrus; PostCent: post-central gyrus; ParaCent: paracentral lobule; PHG: parahippocampal gyrus; Lent: lentiform nucleus; MedFront: medial frontal gyrus; Ling: lingual gyrus; SMG: supramarginal gyrus; Amyg: amygdala; Hipp: hippocampus. FrontoPar: frontoparietal; DorsalAttn: dorsal attention; VentAttn: ventral attention; CingOperc: cingulo-opercular; MedPar: medial parietal; ParOccip: parietal-occipital; NA: not applicable / no network assignment.

Regions with Activity Varying with Maternal Anxiety

Peak in Adult Talairach Space x	y	z	Location	Adult Network	Peak z	Volume (mm^3)	Magnitude greater for higher or lower maternal anxiety?	Not Sig. (p>0.001) After Covariate Control
Regions with Greater Activity for Infants with Higher Maternal Anxiety								
53	-22	24	PostCent	Auditory	9.7	2727	High	ADI, GA, sex, weight, mean FD, retained frames
-50	-43	30	SMG	CingOperc	8.7	2079	High	ADI, sex, depression, stress, state anxiety
-37	-8	-13	PHG	CingOperc	9.9	2673	High	
-37	3	3	Insula	CingOperc	10.4	3267	High	
6	-46	35	Precuneus	CingOperc	8.4	2241	High	
33	5	15	Insula	CingOperc	10.6	3078	High	
44	16	16	IFG	CingOperc	11.0	2538	High	
61	-56	32	SMG	CingOperc	7.0	972	High	
65	-31	26	IPL	CingOperc	12.8	2619	High	
-9	-60	16	PostCing	Default	6.9	1107	High	
-8	30	32	MedFront	Default	4.9	999	High	
1	6	-2	AntCing	Default	7.9	972	High	
3	-56	24	PostCing	Default	11.1	2727	High	
5	-61	41	Precuneus	Default	9.5	3051	High	
6	28	26	Cing	Default	8.4	945	High	
8	40	31	MedFront	Default	6.4	1269	High	
14	-67	20	Cuneus	Default	9.1	2916	High	
16	46	31	SFG	Default	6.3	729	High	
-45	-62	-4	MOG	DorsalAttn	9.7	1809	High	
22	-73	29	Precuneus	DorsalAttn	7.6	2403	High	
22	-67	43	Precuneus	DorsalAttn	8.3	2430	High	
11	-80	34	Cuneus	MedPar	11.8	2916	High	
7	-17	45	ParaCent	MortorHand	6.4	1566	High	
27	-25	24	Insula	MortorHand	7.0	1458	High	
40	-24	45	PostCent	MortorHand	6.2	1890	High	
-36	-44	-40	Tonsil	NA	10.5	1971	High	
-33	-29	27	IPL	NA	5.8	1080	High	
0	-47	-12	Culmen	NA	6.1	918	High	
14	2	29	Cing	NA	7.8	1242	High	
16	-6	36	Cing	NA	6.7	1404	High	
17	-51	28	Cing	NA	9.9	2862	High	
21	-41	20	Cing	NA	8.3	2403	High	
24	17	22	Cing	NA	8.0	1782	High	
28	8	31	IFG	NA	9.1	2268	High	
52	12	37	MFG	NA	9.8	1998	High	
58	-71	14	MTG	NA	8.1	1188	High	
26	-53	16	PostCing	ParOccip	7.6	2349	High	
-39	12	-13	IFG	Unassigned	12.0	2997	High	
-37	2	-22	STG	Unassigned	7.3	1890	High	
-6	30	-19	Rectal	Unassigned	8.7	1674	High	stress

-3	13	-26	Rectal	Unassigned	10.0	837	High	
3	31	-22	Rectal	Unassigned	9.9	2646	High	
36	8	-36	MTG	Unassigned	7.8	1215	High	
47	-29	-28	Fusiform	Unassigned	5.5	891	High	
48	19	-18	STG	Unassigned	8.7	1323	High	
51	11	-11	STG	Unassigned	7.6	1458	High	sex, depression, stress, state anxiety
-54	8	-4	STG	VentAttn	11.4	2241	High	
-47	14	14	IFG	VentAttn	8.2	1107	High	
53	25	4	IFG	VentAttn	8.8	1917	High	
56	17	19	IFG	VentAttn	9.4	2349	High	
-19	-82	7	Cuneus	Visual	7.3	918	High	
-11	-86	19	Cuneus	Visual	9.3	3132	High	
-9	-69	-5	Ling	Visual	7.4	1593	High	
-6	-70	12	Cuneus	Visual	5.9	1107	High	
9	-87	20	Cuneus	Visual	11.7	3186	High	
21	-81	18	Cuneus	Visual	11.1	2754	High	
24	-58	-16	Declive	Visual	7.5	2322	High	
Regions with Greater Activity for Infants with Lower Maternal Anxiety								
-62	-56	28	STG	CingOperc	7.5	891	Low	
-35	6	16	Insula	CingOperc	8.5	1701	Low	
-32	19	9	Insula	CingOperc	8.4	1782	Low	
-29	18	57	MFG	CingOperc	7.4	1404	Low	
31	20	9	Insula	CingOperc	7.7	2349	Low	
43	18	-2	IFG	CingOperc	10.7	2835	Low	
-45	-76	29	MTG	Default	5.7	1107	Low	
20	45	44	SFG	Default	8.7	891	Low	
38	-12	58	PreCent	MortorHand	7.5	2106	Low	
29	-50	-40	Tonsil	NA	7.2	1485	Low	
38	38	38	MFG	NA	8.0	810	Low	
39	-44	-38	Tonsil	NA	7.1	1269	Low	
48	-27	-13	MTG	NA	7.2	891	Low	
62	-58	19	STG	NA	9.6	1539	Low	
-29	25	-4	IFG	Unassigned	4.8	837	Low	
7	45	-22	Orbital	Unassigned	11.3	2403	Low	
20	-18	-35	NA	Unassigned	9.7	1188	Low	
29	22	-5	IFG	Unassigned	9.4	2646	Low	
37	14	-9	IFG	Unassigned	10.4	2484	Low	
52	-2	-22	MTG	Unassigned	9.5	1728	Low	
-61	-61	0	MTG	VentAttn	6.1	783	Low	
-24	-99	-2	Cuneus	Visual	8.8	1647	Low	
-21	-96	-12	Ling	Visual	8.3	1026	Low	
0	-91	3	Cuneus	Visual	7.6	972	Low	
14	-99	6	Cuneus	Visual	10.4	2538	Low	
21	-48	-25	Culmen	Visual	6.8	1512	Low	
30	-88	-10	IOG	Visual	5.7	864	Low	
32	-83	9	MOG	Visual	5.9	1242	Low	
35	-78	-8	MOG	Visual	5.4	891	Low	

TABLE S4. Regions in which activity modulation following the deviant sound varied as a function of maternal trait anxiety. In four regions, the relation between maternal trait anxiety and neonatal brain activity was no longer significant (at a $p<0.001$ level) after controlling for specific covariates; these covariates are listed in the rightmost column for the corresponding regions.

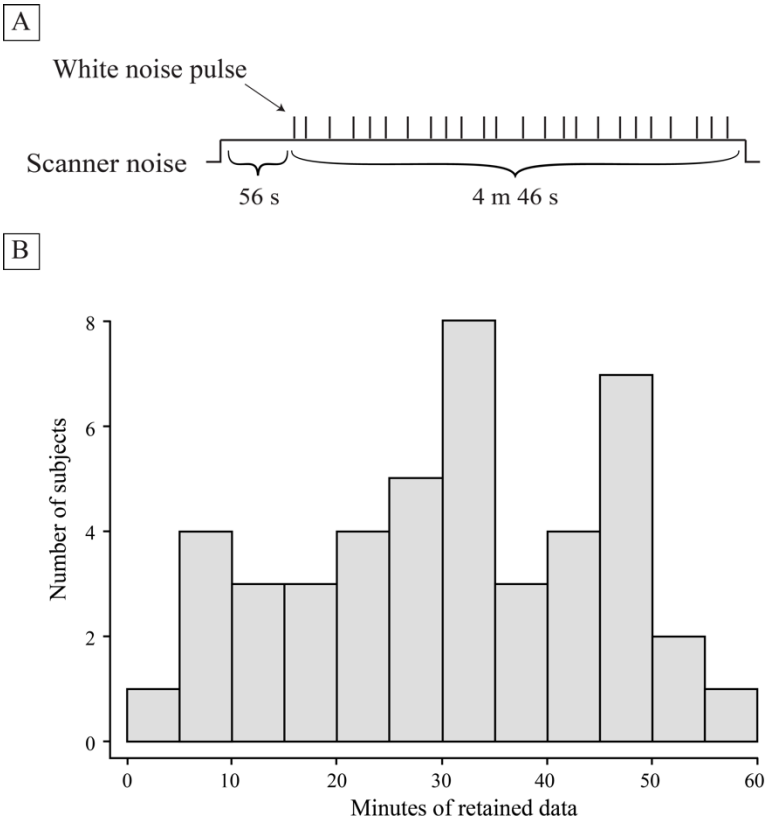

FIGURE S1. Panel A is a schematic of the presentation of the sound stimuli within each fMRI run. BOLD runs were 5.7 minutes in length. Auditory stimuli were 400ms white noise bursts presented every 9-14 seconds in random intervals. Each fMRI run began with a period with no stimuli. In 8 subjects, the run ended with a period with no stimuli (not depicted in the schematic). **Panel B** is a histogram of the amount of data retained per subject after frame censoring.

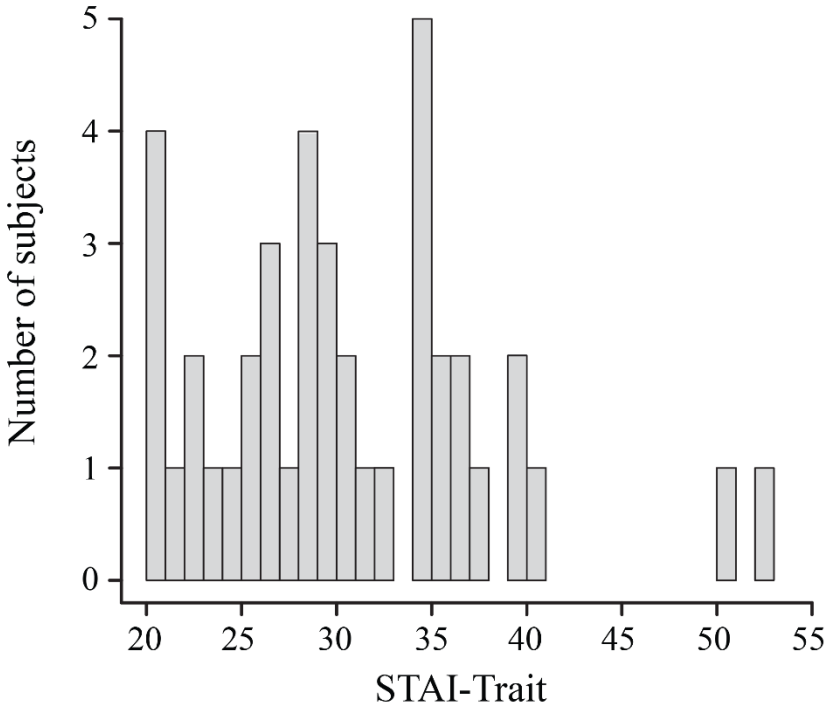

FIGURE S2. Histogram of maternal trait anxiety scores. The two highest scores (values of 51 and 53) were winsorized to the next highest score (41) for analyses incorporating maternal trait anxiety as a continuous measure.

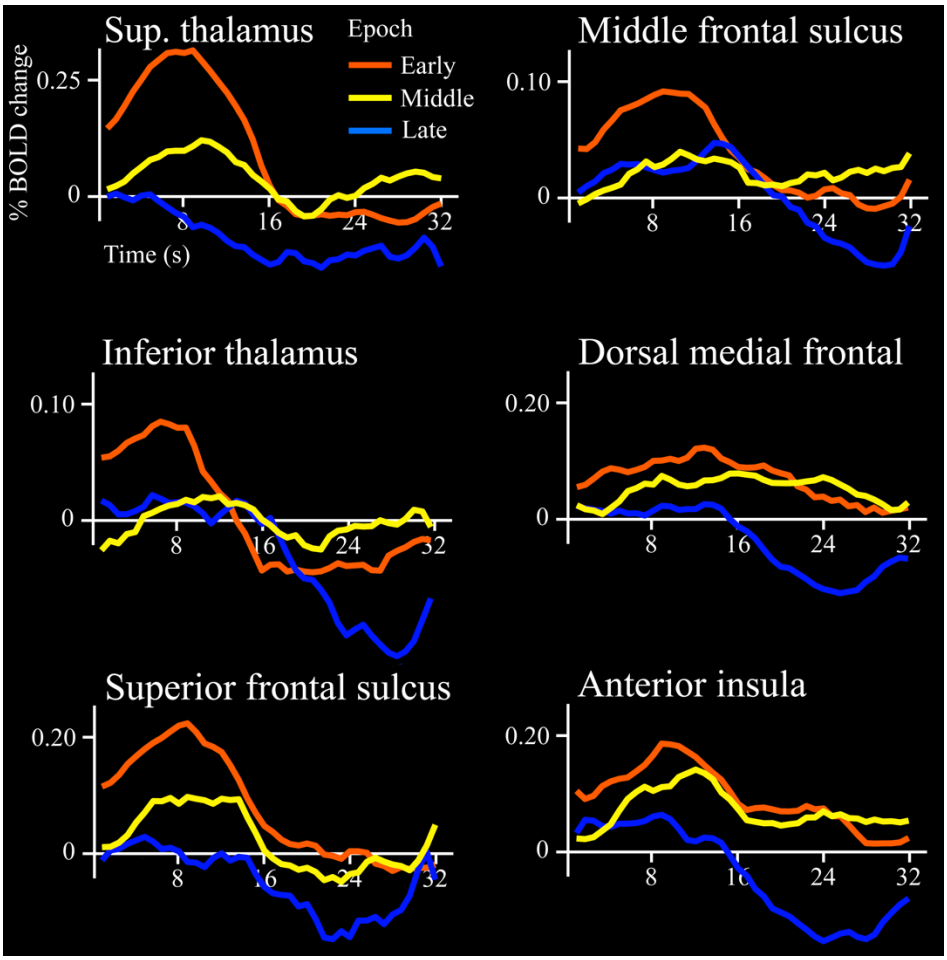

FIGURE S3. In the majority (61%) of brain regions that responded to the auditory stimuli, activity varied significantly between stimuli presented at the beginning, middle, and end of each 5.7 minute BOLD run. In most cases, activity was highest for stimuli presented early in the BOLD runs and lowest for stimuli presented late in the BOLD runs; and generally intermediate for stimuli occurring in the middle of the runs. This figure plots activity for early, middle, and late auditory stimuli in the 6 regions from Figure 1 in the main text in which activity varied significantly as a function of stimulus timing (epoch).

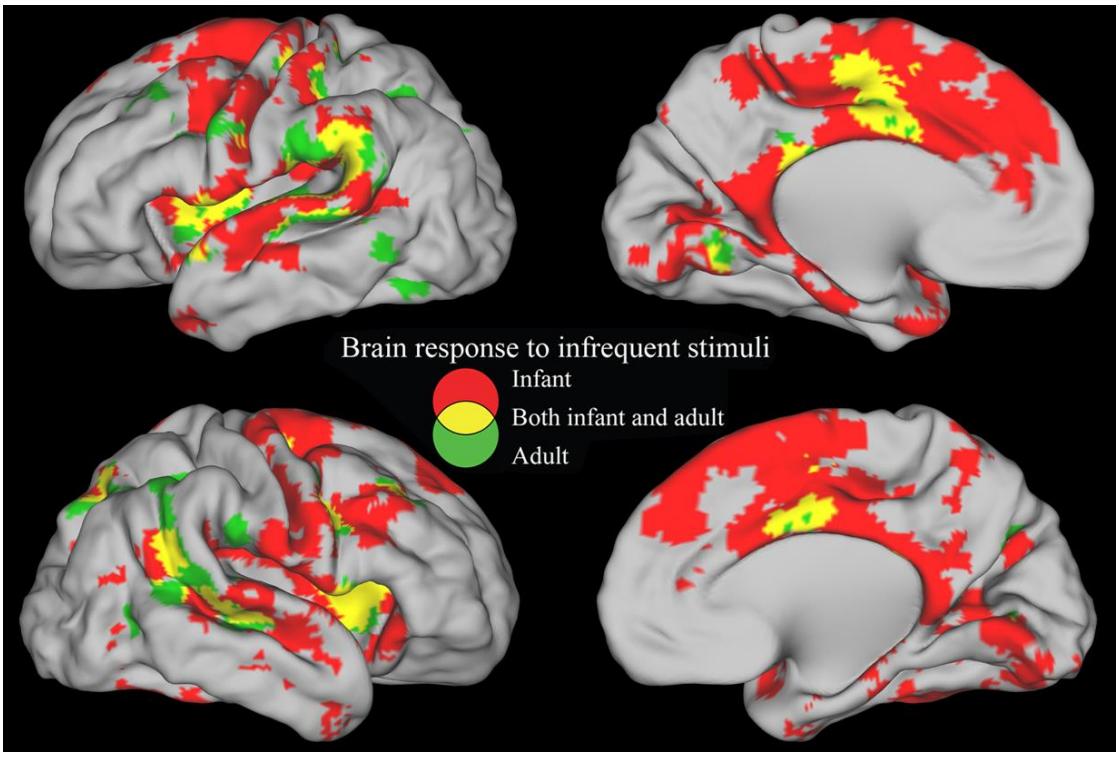

FIGURE S4. Overlap of the neonatal brain response to deviant stimuli from the current study and the adult response to deviant stimuli obtained from a meta-analysis (11). The neonatal areas are regions in which z>3.3, the same data as depicted in the statistical map in Figure 1 in the main text. The adult data were obtained from the author of the adult meta-analysis and are the same data as depicted in Figure 2 from the article describing the meta-analysis (oddball > standard). Nearly all regions from the adult meta-analysis also displayed significant activity in the neonates. Note that while the adult studies report neural response to an oddball relative to a standard tone, we report neural response to an oddball relative to an implicit baseline that includes neural activity evoked by the background scanner noise. The more restricted oddball-related activity in adults relative to neonates is likely to be related to differences in reporting results from meta-analysis (adults) versus results from a single study (neonates); alternatively, there may be a larger representation of deviance in the neonatal brain relative to adults.

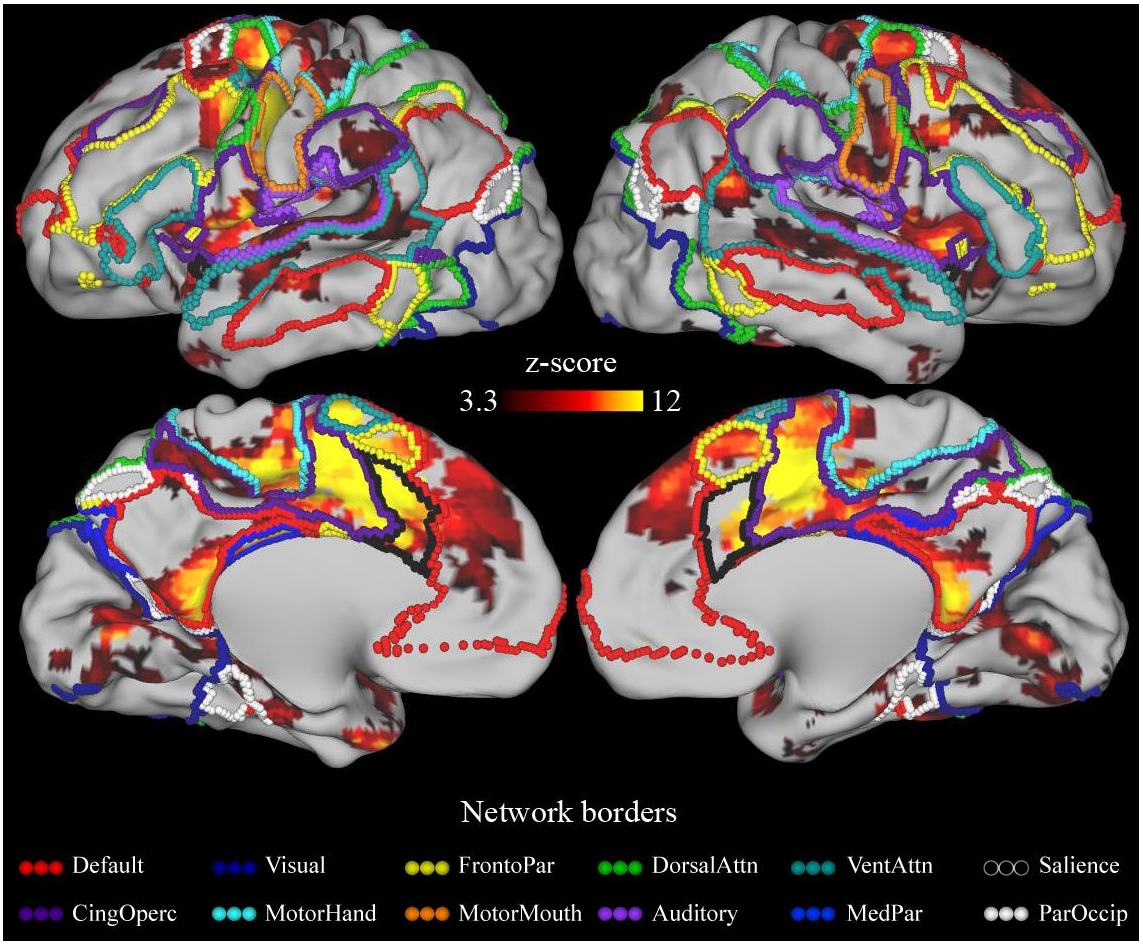

FIGURE S5. Brain areas in which neonatal neural activity modulated following the onset of the deviant sounds, with adult network boundaries overlaid. This figure is identical to Figure 1 in the main text but overlays adult functional network boundaries.

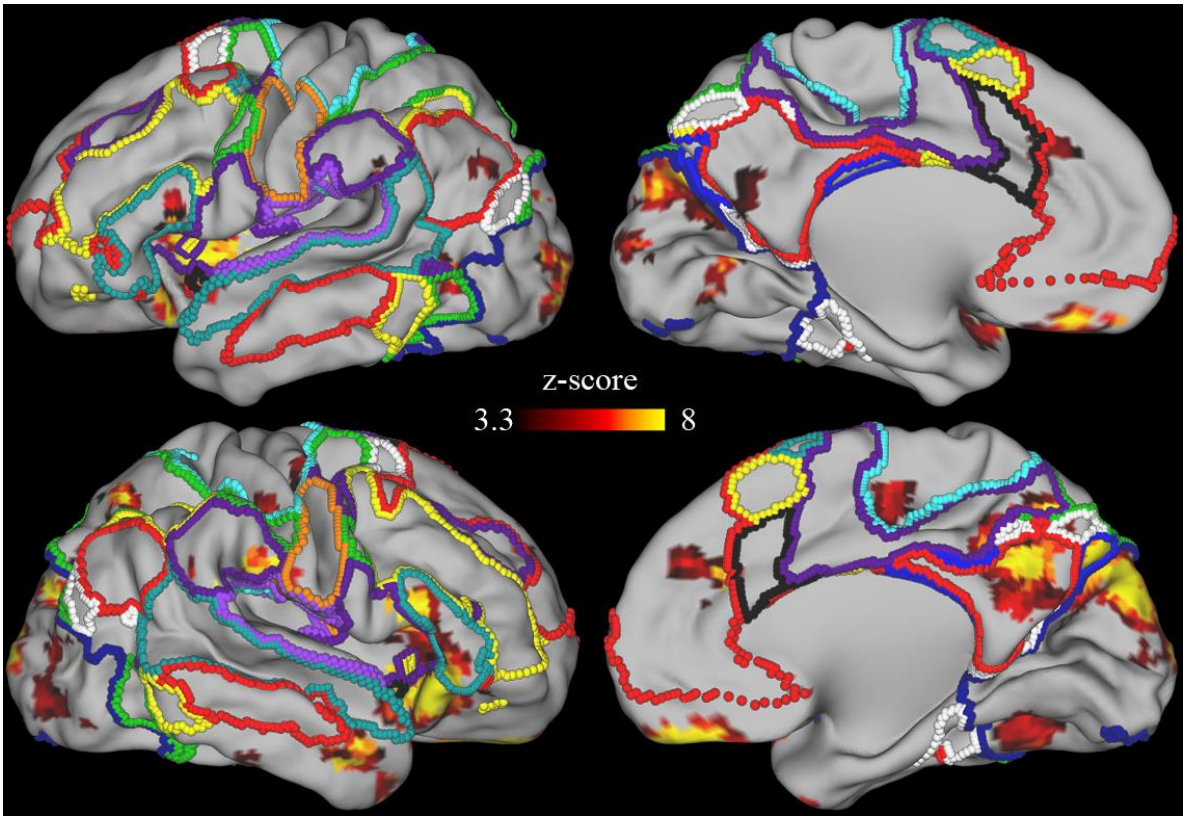

FIGURE S6. Brain regions in which neonatal neural activity following deviant sounds varied as a function of maternal trait anxiety, with adult network boundaries overlaid. This figure is identical to Figure 3 in the main text but overlays adult functional network boundaries.

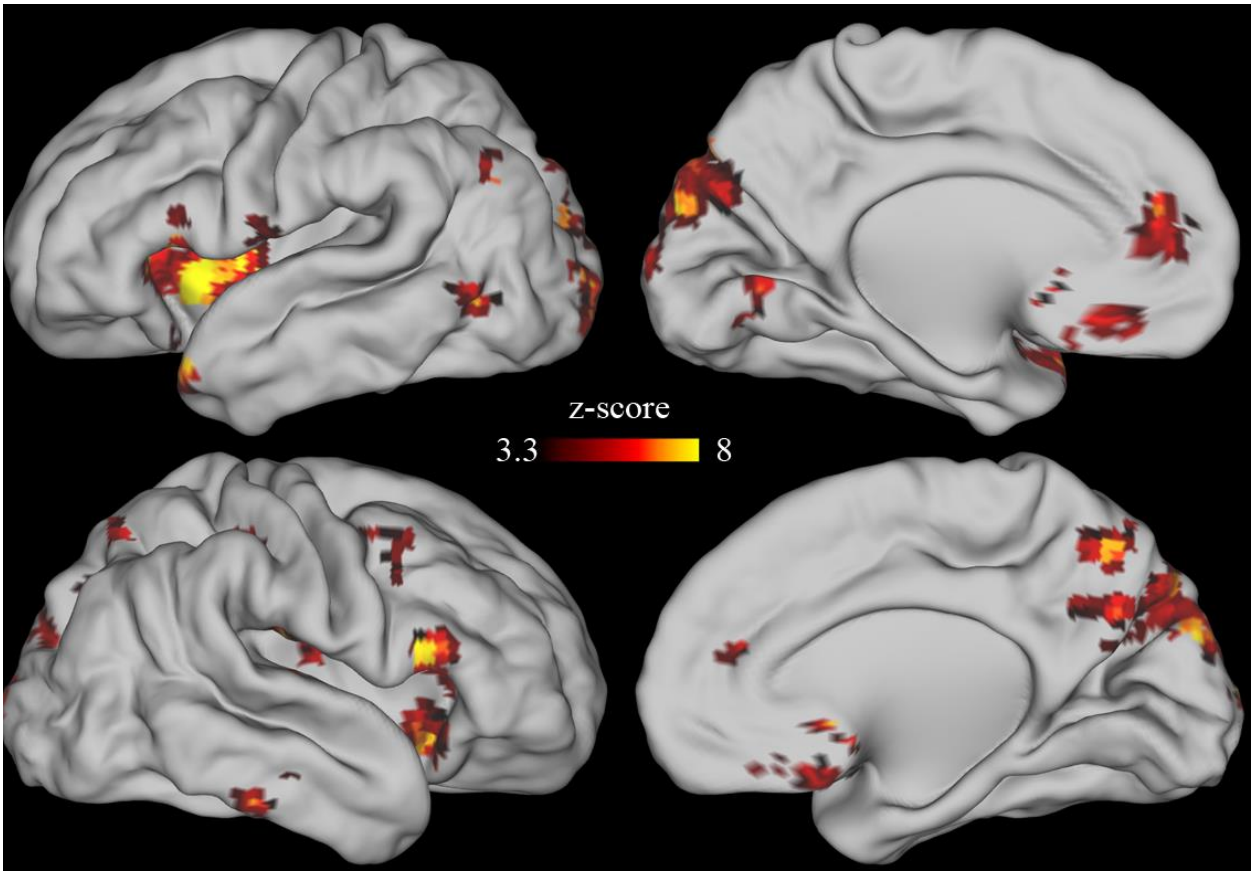

FIGURE S7. Interaction between time and maternal trait anxiety in a model in which maternal trait anxiety is treated as a categorical variable based on median split (higher trait anxiety was STAI-T greater than 30). Results were similar to the model in the main analysis (Figure 3, main text) in which maternal trait anxiety was treated as a continuous variable. The map depicts brain areas in which neonatal neural activity following the onset of deviant sounds varied depending on maternal trait anxiety. Results are whole-brain multiple comparisons corrected at $p<0.01$, with each significant cluster comprised of a volume of at least $756mm^3$ in which each voxel is significant at $p<0.001$.

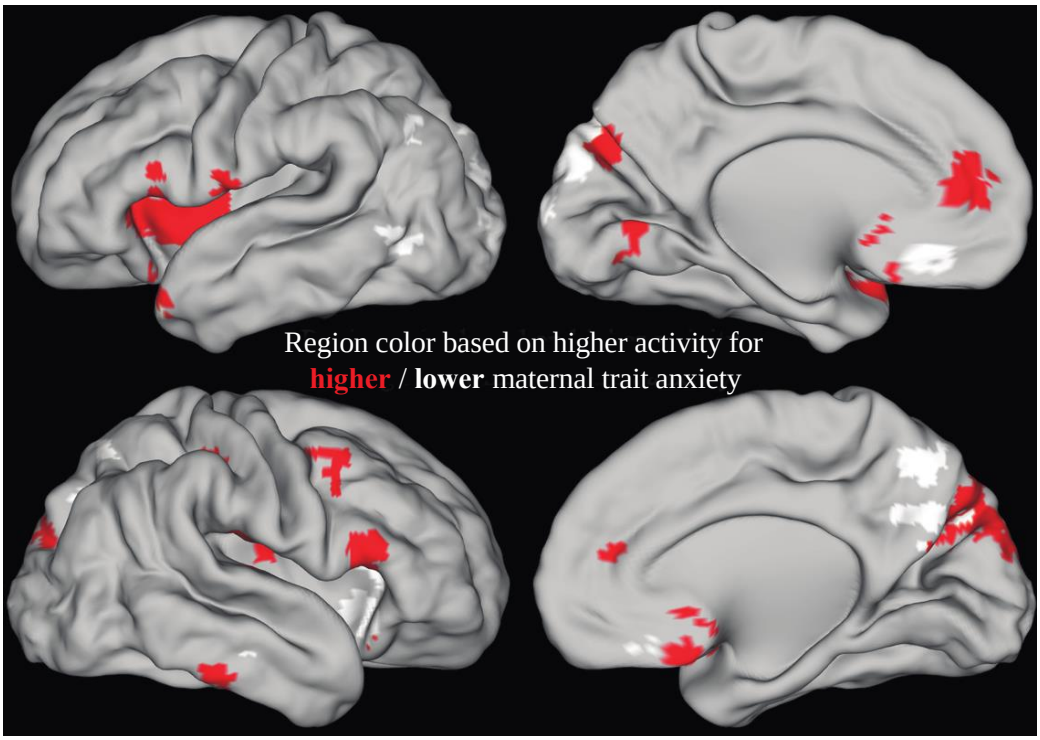

FIGURE S8. Brain regions from Figure S7, in which neonatal neural activity varied as a function of maternal trait anxiety, in a model in which anxiety is categorized into 'higher' or 'lower' based on median split. Areas of cortex in red had higher peak activity in neonates born to mothers with higher trait anxiety, while areas of cortex in white had higher peak activity in neonates born to mothers with lower trait anxiety. Note that the brain regions depicted here are identical to the brain regions in Figure S7 which is a statistical map of the same data.

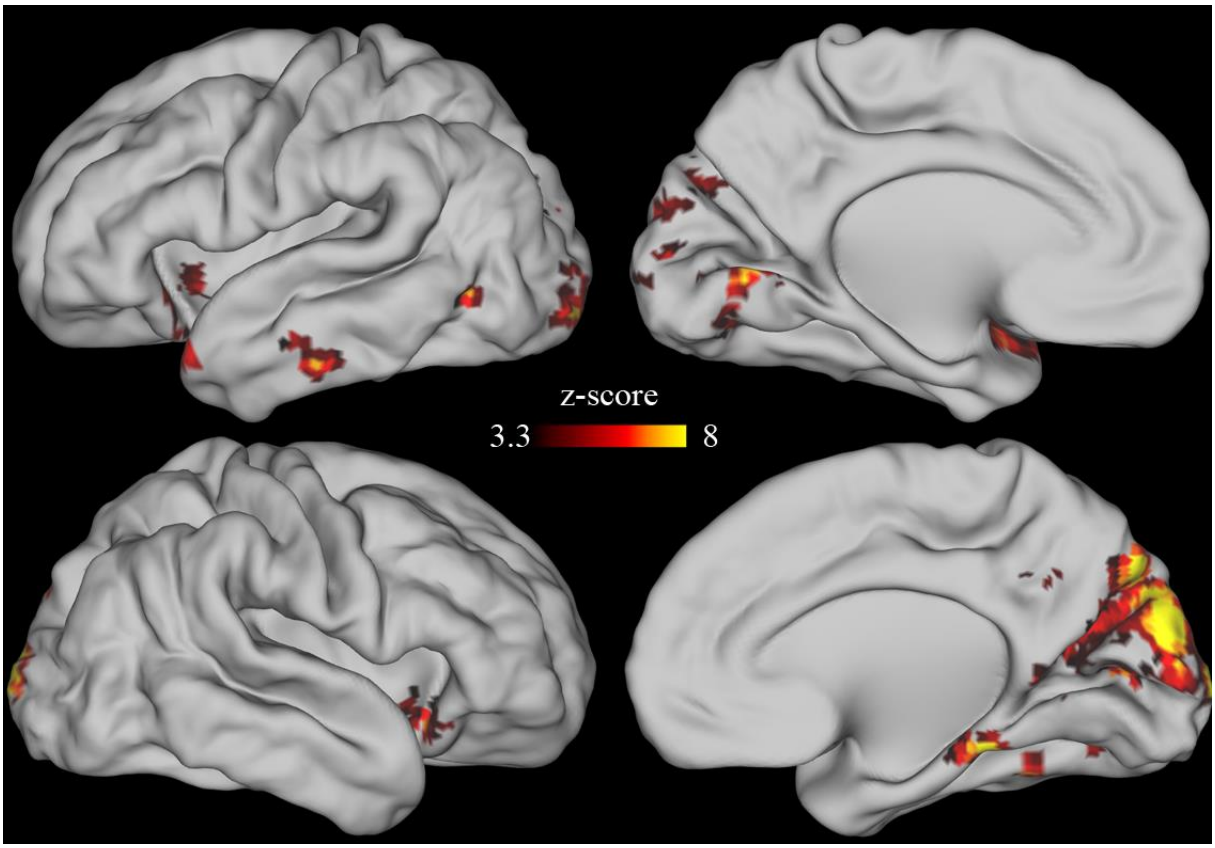

FIGURE S9. Brain areas in which neonatal neural activity following the onset of deviant sounds varied depending on maternal state anxiety (STAI-S). Results are whole-brain multiple comparisons corrected at $p<0.01$, with each significant cluster comprised of a volume of at least $756mm^3$ in which each voxel is significant at $p<0.001$.

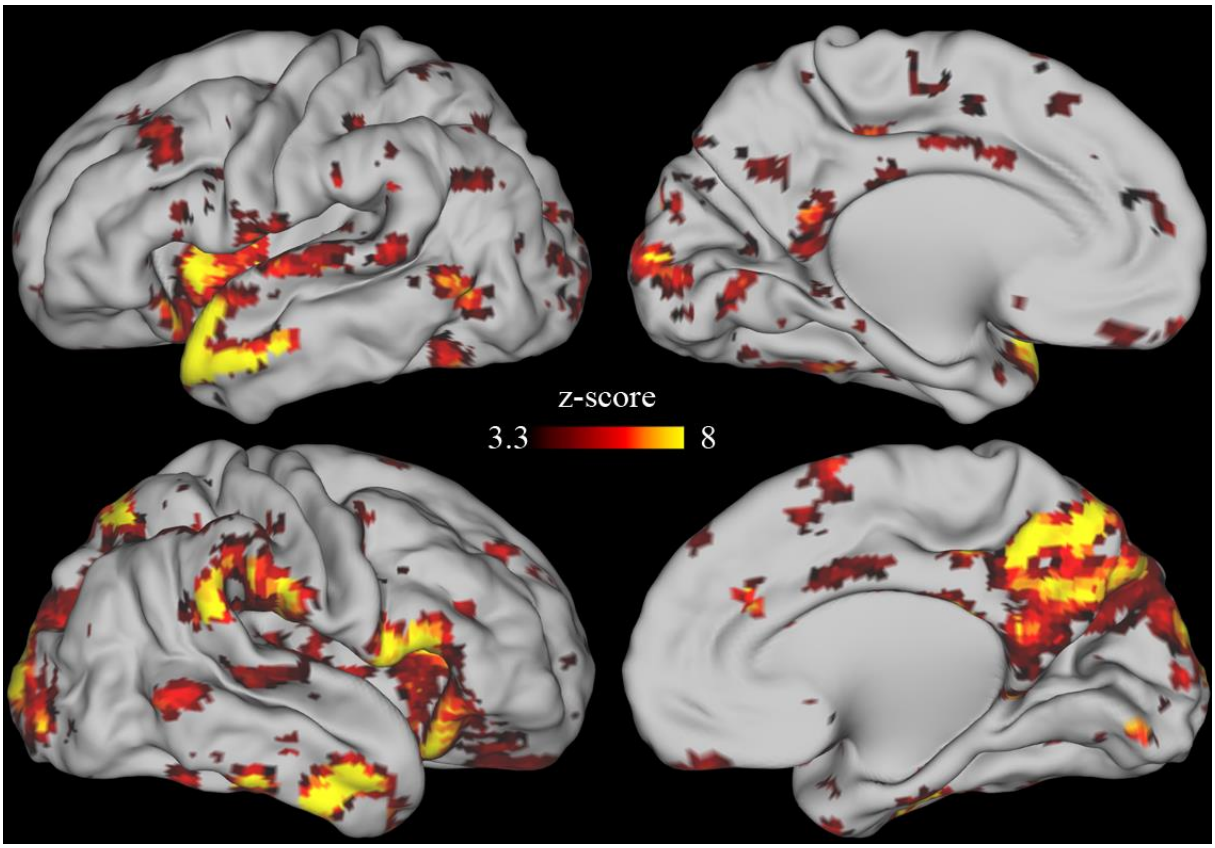

FIGURE S10. Analysis restricted to the n=34 neonates in which maternal trait anxiety was measured in the 5 weeks following birth. This figure displays the interaction between maternal trait anxiety and time. Thus, this map depicts brain areas in which neonatal neural activity following the onset of deviant sounds varied depending on maternal trait anxiety. Results are displayed at a voxelwise threshold of $p<0.001$, uncorrected.

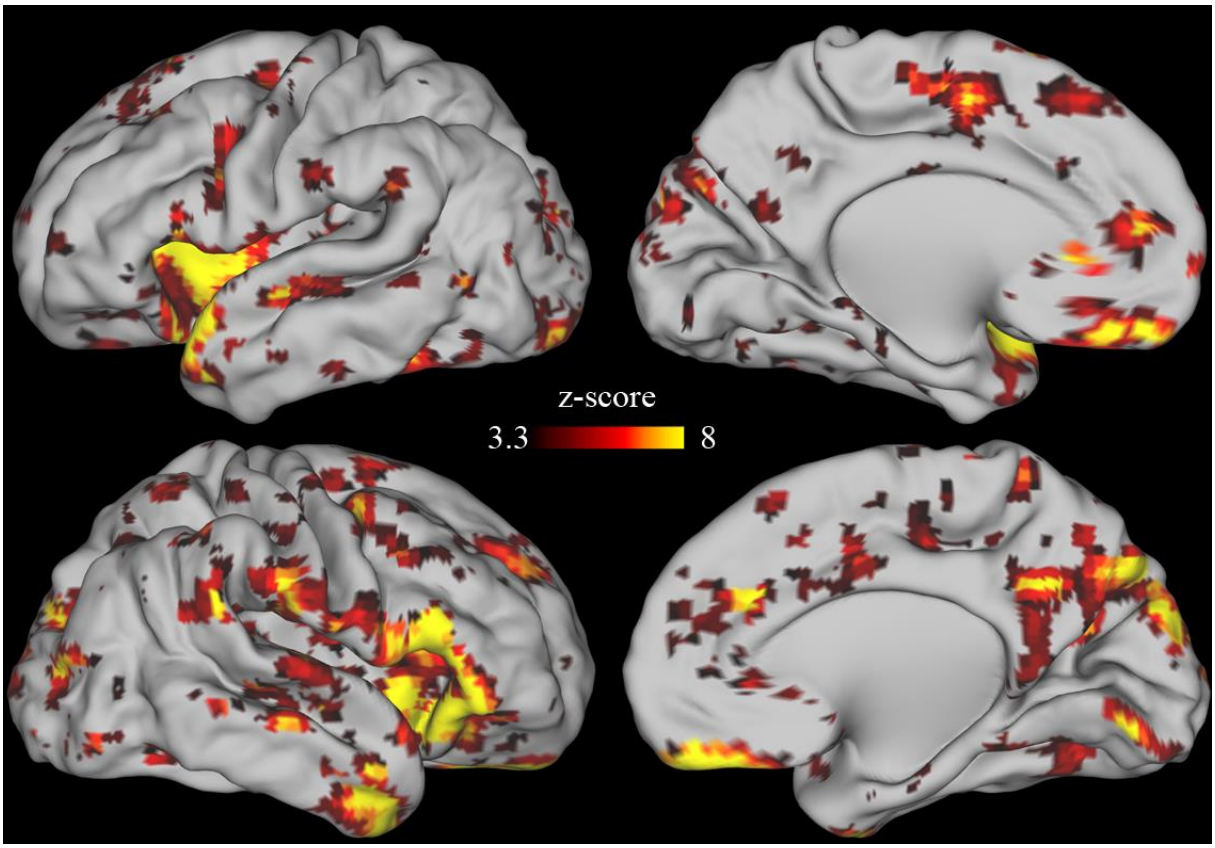

FIGURE S11. Analysis using frame censoring at FD < 0.2. This figure displays the interaction between maternal trait anxiety and time. Thus, this map depicts brain areas in which neonatal neural activity following the onset of deviant sounds varied depending on maternal trait anxiety. Results are displayed at a voxelwise threshold of $p<0.001$, uncorrected.

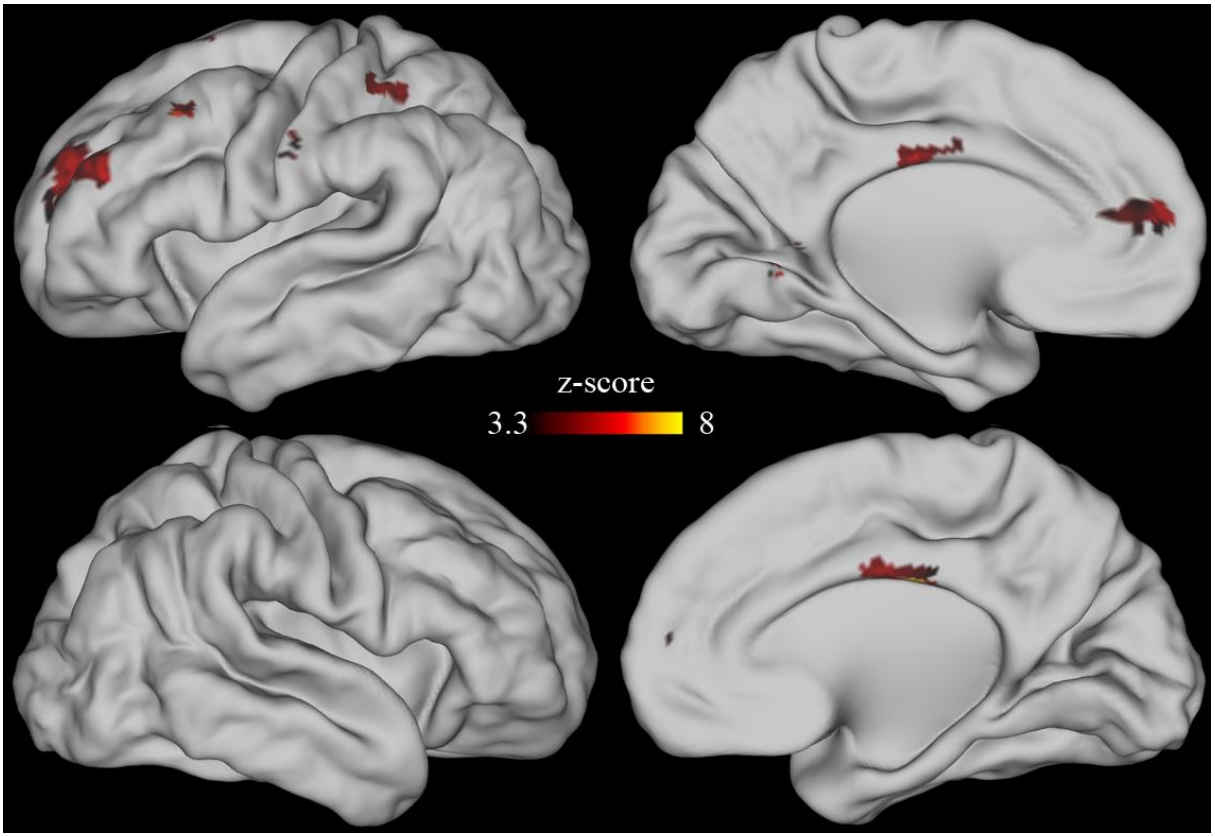

FIGURE S12. Brain regions in which the relation between maternal trait anxiety and neonatal brain activity varied as a function of whether the sound was presented in the beginning, middle, or end of each run (i.e., brain regions with a 3-way interaction between time, maternal trait anxiety, and epoch; see Supplemental Methods for details). Results are whole-brain multiple comparisons corrected at $p<0.01$, with each significant cluster comprised of a volume of at least $756mm^3$ in which each voxel is significant at $p<0.001$.

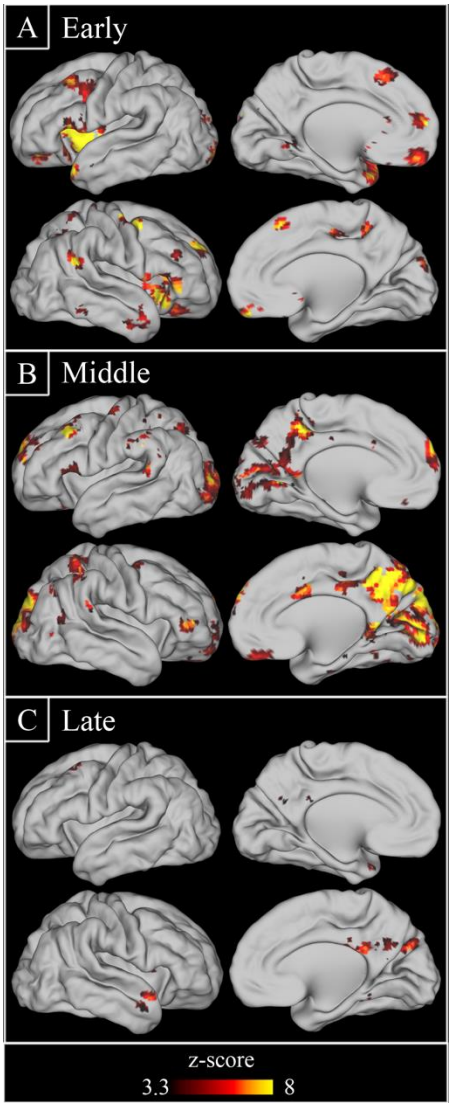

FIGURE S13. Brain regions in which neonatal activity varied as a function of maternal trait anxiety, computed separately for auditory stimuli appearing in the early (first 8 stimuli), middle (next 8 stimuli), or late (last 8 stimuli) epoch of each BOLD run. Results are whole-brain multiple comparisons corrected at $p<0.01$, with each significant cluster comprised of a volume of at least $756mm^3$ in which each voxel is significant at $p<0.001$.

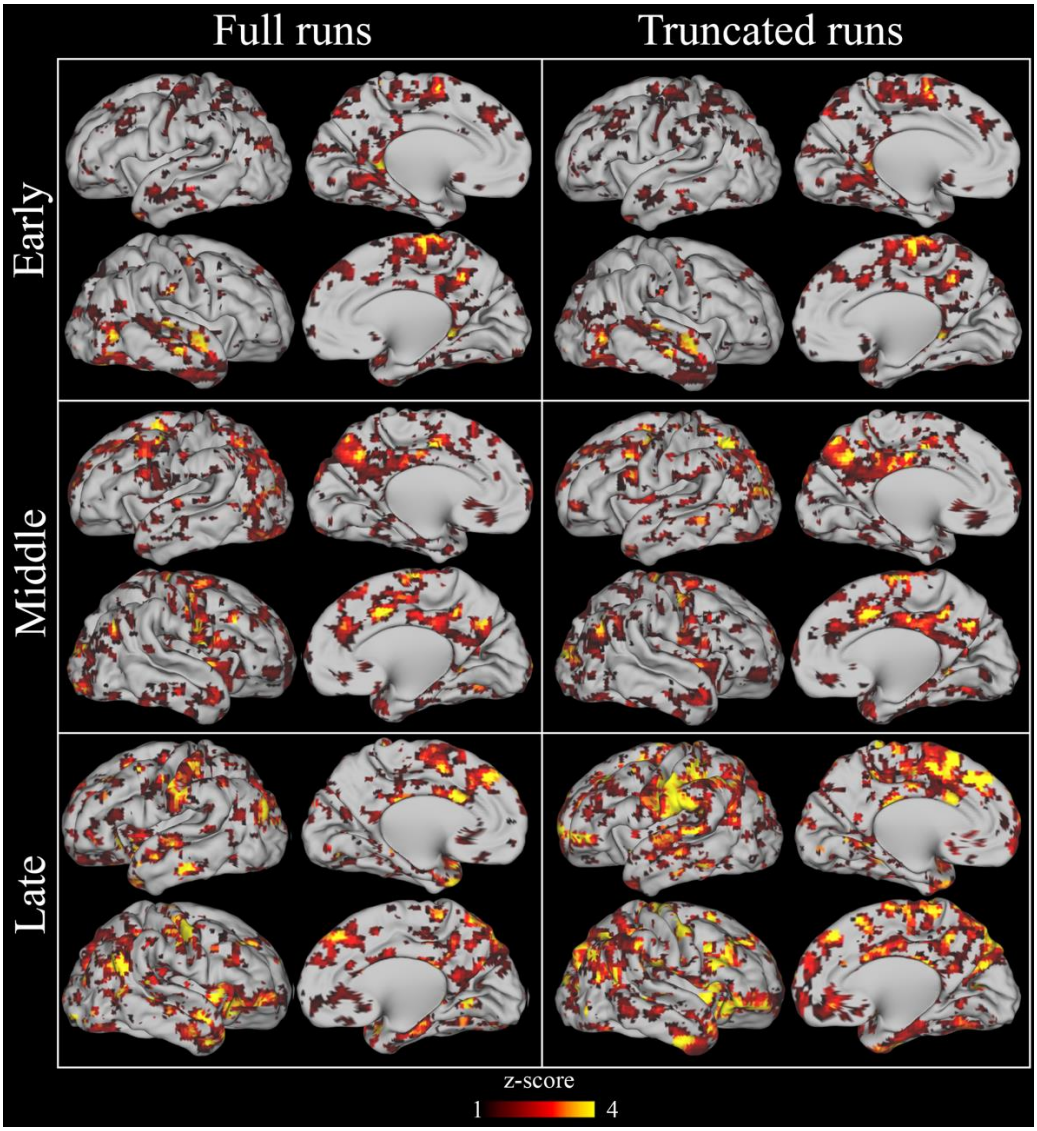

FIGURE S14. Main effect of time image computed solely in the 8 participants who had the extra 56s of scanner noise at the end of each run. These images show parts of the brain that have significant activity modulations following the auditory stimulus. The main effect of time is computed separately from a GLM that did include the extra 56s of data and a GLM that did not include the extra 56s of data. Results are similar, suggesting that the addition of this extra time had little impact on the estimate of the brain activity response.

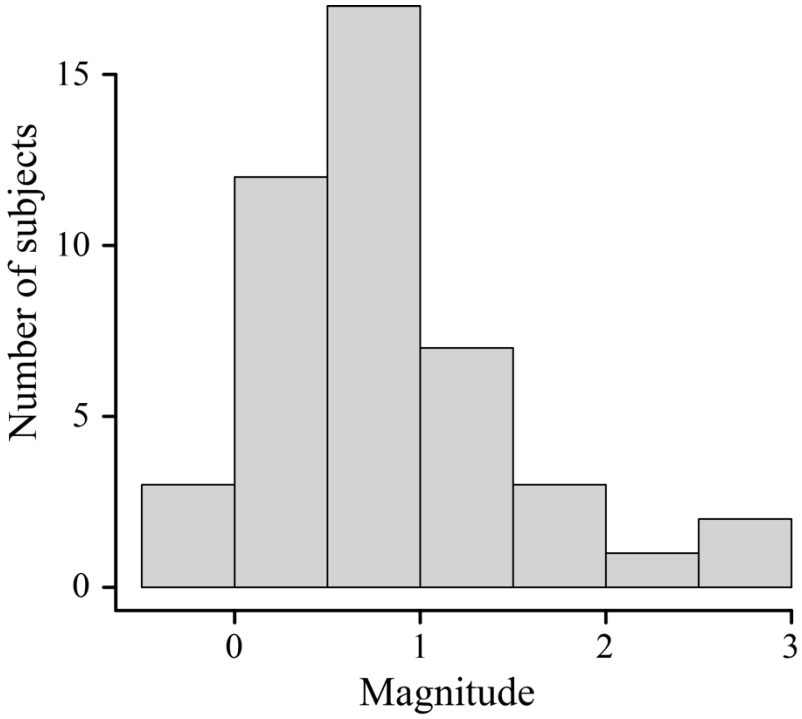

FIGURE S15. Magnitude of maximum regional auditory response in each participant. Magnitudes were derived for each participant in each auditory region from the main effect of time (see Table S3). Magnitudes were computed by taking the dot product of the observed timecourse in a particular region and a 'canonical' hemodynamic response function derived by averaging all timecourses over all regions. As can be seen in the histogram, nearly all participants had evidence of a positive response in auditory cortex.

SUPPLEMENTAL REFERENCES

1. Kind AJH, Buckingham WR. Making Neighborhood-Disadvantage Metrics Accessible - The Neighborhood Atlas. N Engl J Med. 2018;378:2456-2458.
2. Cox JL, Holden JM, Sagovsky R. Detection of postnatal depression. Development of the 10-item Edinburgh Postnatal Depression Scale. Br J Psychiatry. 1987;150:782-786.
3. Cohen S, Williamson G: Perceived stress in a probability sample of the United States. Newbury Park, CA, Sage; 1988.
4. Spielberger CD, Gorsuch RL, Lushene R, Vagg PR, Jacobs GA: Manual for the State-Trait Anxiety Inventory. Palo Alto, CA, Consulting Psychologists Press; 1983.
5. Mathur AM, Neil JJ, McKinstry RC, Inder TE. Transport, monitoring, and successful brain MR imaging in unsedated neonates. Pediatric Radiology. 2008;38:260-264.
6. Cox RW, Chen G, Glen DR, Reynolds RC, Taylor PA. FMRI Clustering in AFNI: False-Positive Rates Redux. Brain connectivity. 2017;7:152-171.
7. Eklund A, Nichols TE, Knutsson H. Cluster failure: Why fMRI inferences for spatial extent have inflated false-positive rates. Proceedings of the National Academy of Sciences of the United States of America. 2016;113:7900-7905.
8. Corbetta M, Patel G, Shulman GL. The reorienting system of the human brain: from environment to theory of mind. Neuron. 2008;58:306-324.
9. Power JD, Mitra A, Laumann TO, Snyder AZ, Schlaggar BL, Petersen SE. Methods to detect, characterize, and remove motion artifact in resting state fMRI. NeuroImage. 2014;84:320-341.
10. Siegel JS, Power JD, Dubis JW, Vogel AC, Church JA, Schlaggar BL, Petersen SE. Statistical improvements in functional magnetic resonance imaging analyses produced by censoring high-motion data points. Human Brain Mapping. 2014;35:1981-1996.
11. Kim H. Involvement of the dorsal and ventral attention networks in oddball stimulus processing: A meta-analysis. Human Brain Mapping. 2013.